Available free online at www.medjchem.com

Mediterranean Journal of Chemistry

Mediterranean Journal of Chemistry **2018**, 7(1), 8-17

Interaction between HSA and a thiosemicarbazide derivative: Analysis of the effect of a methyl group in the binding ability

Otávio Augusto Chaves [1], Margareth Rose de Lima Santos [1], Aurea Echevarria [1], Carlos Mauricio R. Sant'Anna [1], Aurélio B. B. Ferreira [1,*] and José Carlos Netto-Ferreira [1,2,*]

[1] Departamento de Química, Universidade Federal Rural do Rio de Janeiro, BR-465 Km 7, 23970-000 Seropédica-RJ, Brazil

[2] Instituto Nacional de Metrologia, Qualidade e Tecnologia-INMETRO, Divisão de Metrologia Química, 25250-020 Duque de Caxias-RJ, Brazil

Abstract: The interaction between the methyl thiosemicarbazide derivative **ETS2** and Human Serum Albumin (HSA) - the main vehicle of biodistribution of small molecules in the human bloodstream - was evaluated by multiple spectroscopic techniques (circular dichroism, steady state, time-resolved, synchronous and 3D fluorescence) under physiological conditions, combined with theoretical calculations (molecular docking). The interaction HSA:**ETS2** is spontaneous, moderate and is already present in the ground state (static association). Increasing the temperature leads to an increase in binding and the association is entropically driven. The secondary structure of the protein does not suffer significant perturbation upon ligand binding, however, there is a perturbation on the microenvironment around the Trp-214 residue. Sudlow's site I is the main binding site and molecular docking results suggest hydrogen bonding and hydrophobic interactions as the main binding forces. Overall, the presence of the methyl group in the ligand structure does not change significantly the protein structure, however, the presence of this group changed the thermodynamic profile, which strongly suggests that the methyl group decreases the binding ability of the thiosemicarbazide towards serum albumin.

Keywords: Methyl effect; human serum albumin; thiosemicarbazide; spectroscopy; molecular docking.

Introduction

Proteins are the most abundant and versatile macromolecules in living systems and essentially participate in most of the biological processes. Globular proteins, which are usually known to bind to other molecules to form molecular aggregates and to catalyze biochemical reactions, are generally used as functional ingredients in health care and pharmaceutical products [1]. Human Serum albumin (HSA) is one of the main water-soluble proteins in the human bloodstream, accounting for about 60% of the total plasma proteins (42 mg mL^{-1}). Among its functions stands out the biodistribution of different classes of exogenous and endogenous molecules, an important factor in the pharmacokinetic behavior of many drugs [2]. HSA has a molecular mass around 66 KDa and its structure is composed by 585 amino acid residues which form three helical domains (I, II and III) and each domain is comprised of two subdomains (A and B) [3]. The HSA structure has only one tryptophan residue (Trp-214), located in subdomain IIA, also known as Sudlow's site I or warfarin binding site. This amino acid residue is often used for the association studies of albumin with different classes of small molecules by fluorescence spectroscopic techniques [4].

The monovalent methyl group is derived from methane through the removal of a hydrogen atom. Although the methyl group only participates in London dispersion interactions, which are the weakest of all intermolecular interactions, its presence is very important, mainly due to participation in molecular recognition on micromolecules and biomacromolecules, thereby leading to diverse biological effects, including selectivity among bioreceptors. Therefore, the stereoelectronic changes promoted by methyl groups are directly involved in many biological processes [6,7].

Recently, two thiosemicarbazide derivatives were assayed as tyrosinase inhibitors: (*Z*)-2-(3-(phenethyl-amino)-but-2-enoyl)-hydrazine carbothioamide

**Corresponding author: A.B.B. Ferreira, J.C. Netto-Ferreira*
Email address: aureliobf@uol.com.br, jcnetto.ufrrj@gmail.com
DOI: http://dx.doi.org/10.13171/mjc71/01803120918-ferreira

Received February 20, 2017
Accepted, February 27, 2018
Published March 12, 2018

(**ETS1** – Fig. 1) and its methyl derivative (*Z*)-*N*-methyl-2-(3-(phenethylamino)-but-2-enoyl)-hydrazine carbothioamide (**ETS2** – Fig. 1). **ETS1** showed an inhibition percentage of 89.0%, while its methyl derivative showed only 15.0%, suggesting that the methyl group can influence significantly the biological activity towards enzyme tyrosinase. Quantum chemical calculations and molecular docking showed a clear relationship between the HOMO and sulfur electrostatic values of **ETS1** and its efficiency as tyrosinase inhibitor, as well as its better binding ability to Cu^{2+} ions inside the active protein pocket. In addition, the interaction between HSA and **ETS1** was also investigated, indicating a spontaneous and moderate interaction in the site I of the protein, with significant perturbations on the microenvironment around Trp-214 residue [8].

The aim of the present study is to elucidate the methyl effect on the interaction between **ETS2** and HSA, by multiple spectroscopic (circular dichroism, steady state, time-resolved, synchronous and 3D fluorescence) techniques combined with theoretical calculations (molecular docking).

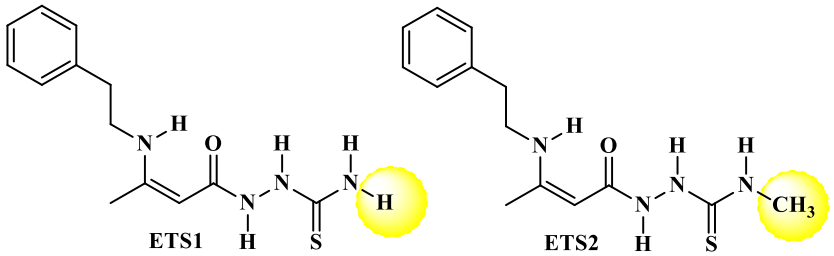

Figure 1. Chemical structure for thiosemicarbazide derivatives **ETS1** and **ETS2**.

Experimental

Materials

Human serum albumin, warfarin, ibuprofen, digitoxin and PBS buffer (pH = 7.4) were purchased from Sigma-Aldrich. Methanol (spectroscopic grade) was purchased from Vetec Química (Brazil). The thiosemicarbazide **ETS2** was synthesized and characterized according to a previous publication [8].

Methodology for spectroscopy measurements

Steady-state fluorescence spectra were measured on a Jasco J-815 spectrometer, in a 1 cm x 1 cm quartz cell, employing a Jasco PFD-425S15F thermostatic cuvette holder. All spectra were recorded with appropriate background corrections. In order to compensate for the inner filter effect from **ETS2**, the fluorescence intensity was corrected at λ = 280 nm and 340 nm, according to equation 1[9]:

$$F_{cor} = F_{obs} 10^{[(A_{ex}+A_{em})/2]} \quad (1)$$

where F_{cor} and F_{obs} are the corrected and observed fluorescence intensity values, respectively. A_{ex} and A_{em} are the experimental absorbance values at the excitation (ε = 9247 $M^{-1}cm^{-1}$ in PBS at 280 nm) and emission wavelengths (ε = 1215 $M^{-1}cm^{-1}$ in PBS at 340 nm), respectively.

Steady-state fluorescence spectra were measured in the 300-450 nm range, at 296 K, 303 K and 310 K, with excitation wavelength at 280 nm. Firstly, the spectrum for a 3.0 mL solution containing HSA ($1.00x10^{-5}$ M, in PBS solution at pH = 7.4) was recorded. Then, the fluorescence emission spectrum of solutions resulting from successive addition of aliquots from a stock solution of **ETS2** ($1.00x10^{-3}$ M, in methanol) with final concentrations of 0.17; 0.33; 0.50; 0.66; 0.83; 0.99; 1.15 and $1.32x10^{-5}$ M were also recorded.

Time-resolved fluorescence measurements were performed on a spectrofluorimeter model FL920 CD, from Edinburgh Instruments, equipped with an EPL laser (λ_{exc} = 280±10 nm; the pulse of 850 ps and energy of 1.8 μW/pulse) and monitoring emission at 340 nm. Fluorescence decay was obtained for the free HSA solution ($1.00x10^{-5}$ M at pH = 7.4) and for an HSA solution containing the maximum concentration of **ETS2** used in the steady-state fluorescence studies ($1.32x10^{-5}$ M), at room temperature (*ca* 298 K).

Synchronous fluorescence (SF) and 3D fluorescence spectra were obtained from a spectrofluorimeter model Xe900 from Edinburgh Instruments. SF spectra for HSA ($1.00x10^{-5}$ M) were recorded with increasing concentrations of **ETS2**, in the same concentration range used in the steady-state fluorescence studies. The spectra were recorded in the 240–320 nm range by setting Δλ=60 nm and Δλ = 15 nm for tryptophan and tyrosine residues, respectively, at room temperature (*ca* 298 K). 3D fluorescence spectra of HSA were recorded in the absence and presence of **ETS2**, using an excitation wavelength range of 200–340 nm and emission wavelength range of 210-460 nm, at room temperature (*ca* 298 K). 3D spectra were recorded for 3.0 mL of HSA solution ($1.00x10^{-5}$ M, at pH=7.4) and for HSA:**ETS2** in the maximum concentration of quencher used in the steady-state fluorescence measurements ($1.32x10^{-5}$ M).

Competitive binding studies were carried out employing three different probes: warfarin, ibuprofen or digitoxin. HSA and site probes were used at a fixed concentration ($1.00x10^{-5}$ M) and fluorescence

quenching titration with **ETS2** was performed as described previously in the steady-state fluorescence quenching methodology, at 310 K.

Circular dichroism (CD) spectra were measured on a Jasco J-815 spectrometer, in a 1 cm x 1 cm quartz cell, employing a Jasco PFD-425S15F thermostatic cuvette holder. All spectra were recorded with appropriate background corrections. CD spectra were measured in the 200-260 nm range for HSA ($1.00x10^{-6}$ M at pH = 7.4) and HSA:**ETS2** with a ligand concentration of $1.32x10^{-5}$ M at 310 K. The CD results were expressed in terms of significant molar residual ellipticity (MRE) in $degcm^2dmol^{-1}$, according to equation 2:

$$MRE = \frac{\theta}{(10.n.l.C_p)} \quad (2)$$

where Θ is the observed CD (in milli-degrees), n is the number of amino acid residues (585 for HSA) [10] l is the path length of the cell (in cm) and C_p is the molar concentration of HSA ($1.00x10^{-6}$ M).

In order to investigate possible perturbation on HSA structure in the presence of methanol-solvent used for **ETS2** -, steady-state fluorescence and circular dichroism spectra of HSA were recorded without and in the presence of 40 µL of methanol and no significant effect was observed.

Methodology for molecular docking calculations

The crystallographic structure of HSA was obtained from the Protein Data Bank (PDB) with access code 1N5U[11]. The thiosemicarbazide **ETS2** structure was built and energy-minimized with the Density Functional Theory (DFT) method Becke-3-Lee Yang Parr (B3LYP) with the standard 6-31G* basis set available in the Spartan '14 program (Wavefunction, Inc.).

Molecular docking was performed with the GOLD 5.2 program (CCDC). Hydrogen atoms were added to the protein according to the data inferred by the program on the ionization and tautomeric states. Docking interaction cavities explored for the docking procedure were delimited by a 10 Å radius from the Trp-214 residue. The number of genetic operations (crossover, migration, mutation) in each docking run used in the searching procedure was set to 100,000 and during each docking run the amino acid residues were considered as static. The program optimizes hydrogen-bond geometries by rotating hydroxyl and amino groups of the amino acid side chains. The scoring function used was '*ChemPLP*', which is the default function of the GOLD 5.2 program [12]. For more details on molecular docking procedure, see previous publications [4,9].

Results and Discussion

Binding ability between HSA and ETS2

Fluorescence spectroscopic techniques are essential research devices in biochemistry and biophysics, used to measure protein-drug interactions. A number of molecular interactions can result in a quenching process, which can include excited state reaction, molecular rearrangements, ground-state complex formation, collisional quenching, etc [13]. The fluorescence spectra of HSA in the absence and presence of **ETS2** are given in Fig. 2. The maximum fluorescence emission of HSA (340 nm) decreases upon successive additions of **ETS2** indicating that the ligand should be located near the Trp-214 residue [4].

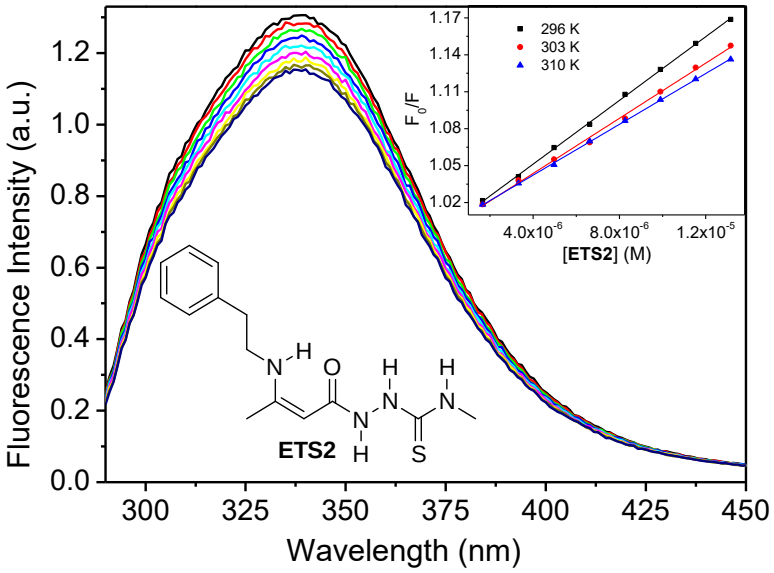

Figure 2. Fluorescence emission spectra for HSA and its fluorescence quenching upon successive addition of **ETS2** at pH = 7.4 and 310 K. *Inset:* Stern-Volmer plots for the interaction between HSA:**ETS2** at 296 K, 303 K and 310 K. [HSA] = $1.00x10^{-5}$ M and [**ETS2**] = 0.17; 0.33; 0.50; 0.66; 0.83; 0.99; 1.15 and $1.32x10^{-5}$ M.

In order to identify the main fluorescence quenching mechanism (static and/or dynamic), Stern-Volmer analysis were applied according to equation 3 [14]:

$$\frac{F_0}{F} = 1 + k_q \tau_0 [Q] = 1 + K_{SV}[Q] \quad \text{(A)} \qquad k_q = \frac{K_{SV}}{\tau_0} \quad \text{(B)} \qquad (3)$$

where F_0 and F are the fluorescence intensity of the protein sample in the absence and presence of the quencher, respectively. K_{SV} and k_q are the Stern-Volmer constant and the bimolecular quenching rate constant, respectively. [Q] is the **ETS2** concentration and τ_0 is the lifetime of the Trp-214 residue in the absence of quencher - the measured mean value for the fluorescence lifetime of HSA was (5.78±0.13)x10^{-9} s.

A Stern-Volmer plot for the fluorescence quenching of HSA by the addition of successive aliquots of **ETS2** is shown in the *inset* of Fig. 2. K_{SV} values decrease with the temperature increase and the k_q values are of the order of 10^{12} M^{-1}s^{-1} (Table 1), being larger than the maximum scattering collision quenching constant ($k_{diff} \approx 2.00\text{x}10^{10}$ M^{-1}s^{-1}) [15], indicating that the fluorescence quenching must be occurring *via* a static process. Thus, there is a non-fluorescent association between the fluorophore (Trp-214 residue) and thiosemicarbazide **ETS2** in the ground state[16].

In order to further confirm which type of fluorescence quenching mechanism is involved in the HSA: **ETS2** interaction, time-resolved fluorescence measurements were carried out for HSA without and in the presence of the ligand. The main HSA fluorophore is the Trp-214 residue, which showed two main fluorescence lifetimes (Fig. 3): τ_1 = 1.86±0.16 ns with a 21.2% contribution and τ_2 = 5.78±0.13 ns with a 78.8% contribution (χ^2 = 1.175), in full agreement with literature results [17]. In the presence of **ETS2,** the HSA fluorescence lifetimes were τ_1 = 1.84±0.15 ns with a 22.6% contribution and τ_2 = 5.74±0.11 ns with a 77.4% contribution (χ^2 = 1.152). Since the fluorescence lifetimes of free HSA and HSA associated with **ETS2** are the same, within the experimental error, it can be concluded that the fluorescence quenching mechanism is static, which implies a ground-state association between the tryptophan residue in HSA and **ETS2**. These results are in total accordance with those shown above for the steady-state fluorescence quenching (ground-state association, Table 1) [18,19]. The same trend was reported for the thiosemicarbazide **ETS1** [8], from which it can be concluded that the presence of the methyl group in the ligand **ETS2** structure does not change the fluorescence quenching mechanism

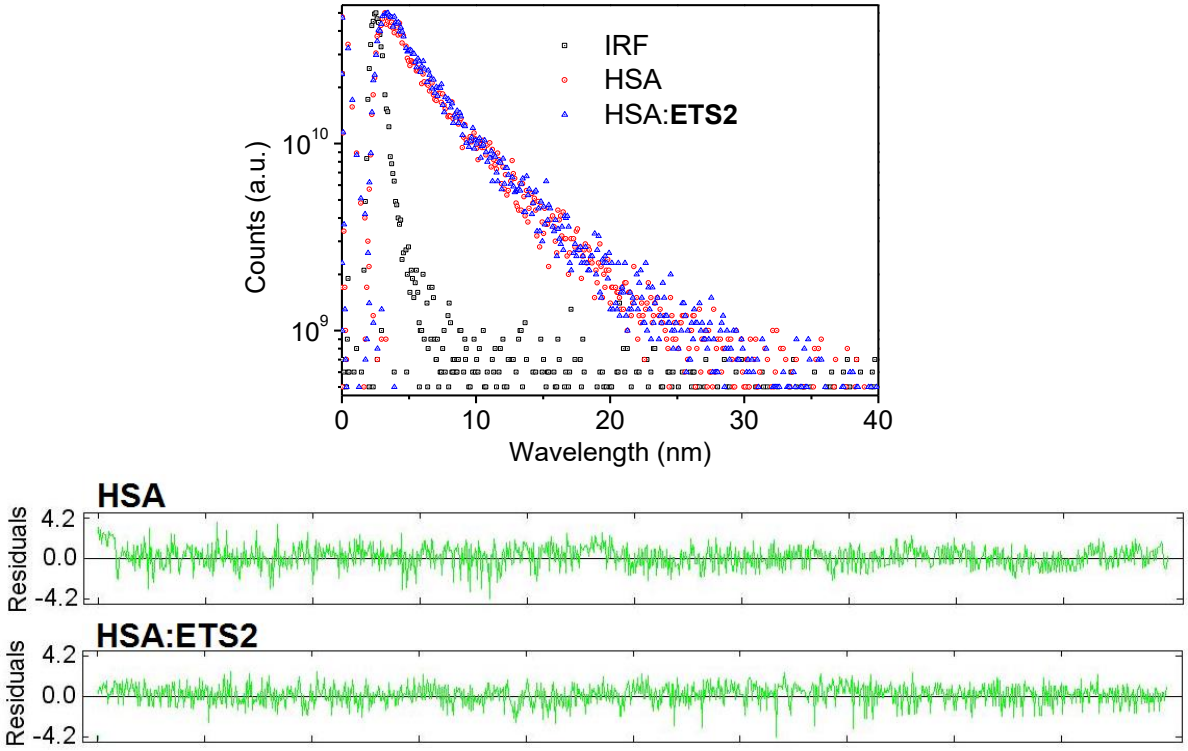

Figure 3. Time-resolved fluorescence decay and its residuals for HSA solution and HSA:**ETS2** at pH = 7.40 and 310 K. [HSA] = 1.00x10^{-5} M and [**ETS2**] = 1.32x10^{-5} M, at room temperature.

For a static quenching process, the modified Stern-Volmer analysis can be applied to determine the binding constant between HSA and the thiosemicarbazide under study – Fig. 4 and equation 4 [19]:

$$\frac{F_0}{F_0 - F} = \frac{1}{f[Q]K_a} + \frac{1}{f} \quad (4)$$

where F_0 and F are the fluorescence intensity of the protein sample in the absence and in the presence of the quencher, respectively. K_a is the modified Stern-Volmer binding constant; f is the fraction of the initial fluorescence intensity that corresponds to the fluorophore that is accessible to the quencher and [Q] the **ETS2** concentration.

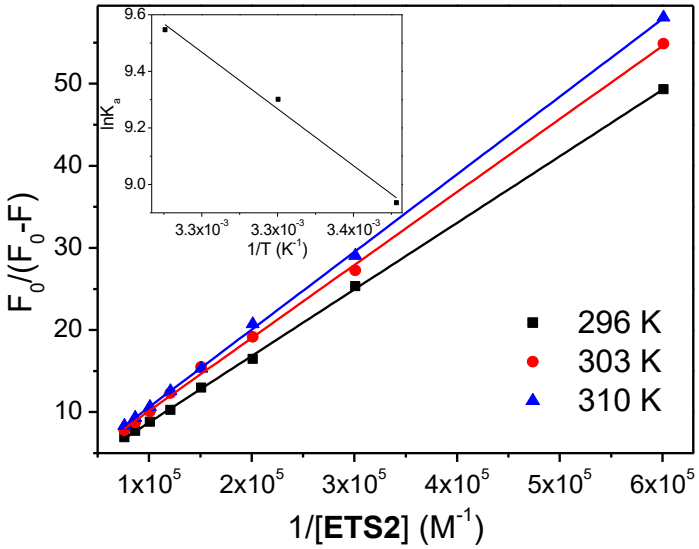

Figure 4. Modified Stern-Volmer plots for the interaction HSA: **ETS2** at pH = 7.4 and three different temperatures. *Inset*: Van't Hoff plot for the interaction HSA: **ETS2**. [HSA] = 1.00x10^{-5} M and [**ETS2**] = 0.17; 0.33; 0.50; 0.66; 0.83; 0.99; 1.15 and 1.32x10^{-5} M.

As can be seen in Table 1, the K_a values are of the order of 10^4 M^{-1}, indicating a moderate interaction between HSA and **ETS2** [4,19,20]. The increase in K_a values with increasing temperature, suggests that at higher temperatures the increased mobility inside the serum albumin structure allows **ETS2** to find improved binding within the protein pocket. This result is the opposite for **ETS1** [8], suggesting that the presence of the methyl group in the thiosemicarbazide structure can stabilize the ligand binding at a higher temperature, probably due to an hydrophobic interaction between the methyl group and the amino acid residues present in the protein pocket.

In general, four representative interaction forces, namely hydrophobic force, hydrogen bond, van der Waals force, and electrostatic interactions, exist between small molecules and biological macromolecules and thermodynamic parameters (enthalpy change - $\Delta H°$ - and entropy change - $\Delta S°$) can be used as evidence to identify the main binding forces between ligand and protein. In order to determine $\Delta H°$ and $\Delta S°$ values for the association between HSA and **ETS2**, the van't Hoff analysis (*inset* in Fig. 4 and equation 5A) can be applied [21]. In addition, the spontaneity of the binding process can be calculated with Gibb's free energy equation (equation 5B):

(A) (B) (5)

$$\ln K_a = -\frac{\Delta H^0}{RT} + \frac{\Delta S^0}{R} \qquad \Delta G^0 = \Delta H^0 - T\Delta S^0$$

where K_a is the modified Stern-Volmer binding constant at the corresponding temperature, R represents the gas constant (8.314x10^{-3} kJmol^{-1}K^{-1}), T is the temperature (296 K, 303 K and 310 K) and $\Delta G°$, $\Delta H°$ and $\Delta S°$ are Gibb's free energy, enthalpy and entropy changes, respectively.

Table 1 shows negative $\Delta G°$ values for HSA:**ETS2**, which is in accordance with the spontaneity of the binding process. In this case, only the entropy change value is responsible for the major contribution to the negative sign of $\Delta G°$, indicating that the interaction HSA:**ETS2** is entropically driven [9]. For the sample without the methyl group, the binding was enthalpically and entropically driven [8].

Table 1. Stern-Volmer constants (K_{SV}), quenching rate constants (k_q), modified Stern-Volmer binding constants (K_a) and thermodynamic parameters ($\Delta H°$, $\Delta S°$ and $\Delta G°$) for the interaction HSA:**ETS2**.

Code	T (K)	K_{SV} (x10^4) (M^{-1})	k_q (x10^{12}) ($M^{-1}s^{-1}$)	r^2	K_a (x10^4) (M^{-1})	r^2	$\Delta H°$ (kJmol^{-1})	$\Delta S°$ (kJmol^{-1}K^{-1})	$\Delta G°$ (kJmol^{-1})	r^2
ETS2	296	1.29±0.01	2.24	0.9994	0.76±0.03	0.9997			-22.0	
	303	1.12±0.02	1.94	0.9971	1.10±0.26	0.9990	33.4±3.3	0.187±0.011	-23.3	0.9804
	310	1.00±0.01	1.79	0.9996	1.40±0.26	0.9996			-24.6	

Ross and Subramanian have characterized the sign of the thermodynamic parameters with various kinds of interaction which may take place in the protein association process [22]. Table 1 shows that both $\Delta H°$ and $\Delta S°$ values are positive, indicating hydrogen bonding and hydrophobic interactions as the main binding forces in the binding process. From the standpoint of water structure, positive entropy is often regarded as a typical signature of hydrophobic interactions, since the water molecules which are arranged in an orderly fashion around the ligand and the protein molecules acquire a more random configuration as a result of hydrophobic interactions [16].

Conformational investigation of HSA without and in the presence of ETS2

In order to determine the presence of a possible perturbation on the secondary structure of the albumin upon **ETS2** binding, circular dichroism (CD) experiments were carried out at pH = 7.4 and 310 K. The CD spectrum of HSA exhibited two negative bands in the UV region, which are characteristic of the α-helical structure: 208 (π-π* transition) and 222 nm (*n*-π* transition) [10]. Fig. 5A shows a clear decrease in the CD signal upon the addition of **ETS2**, indicating that there is a perturbation on the secondary structure of the albumin upon ligand binding.

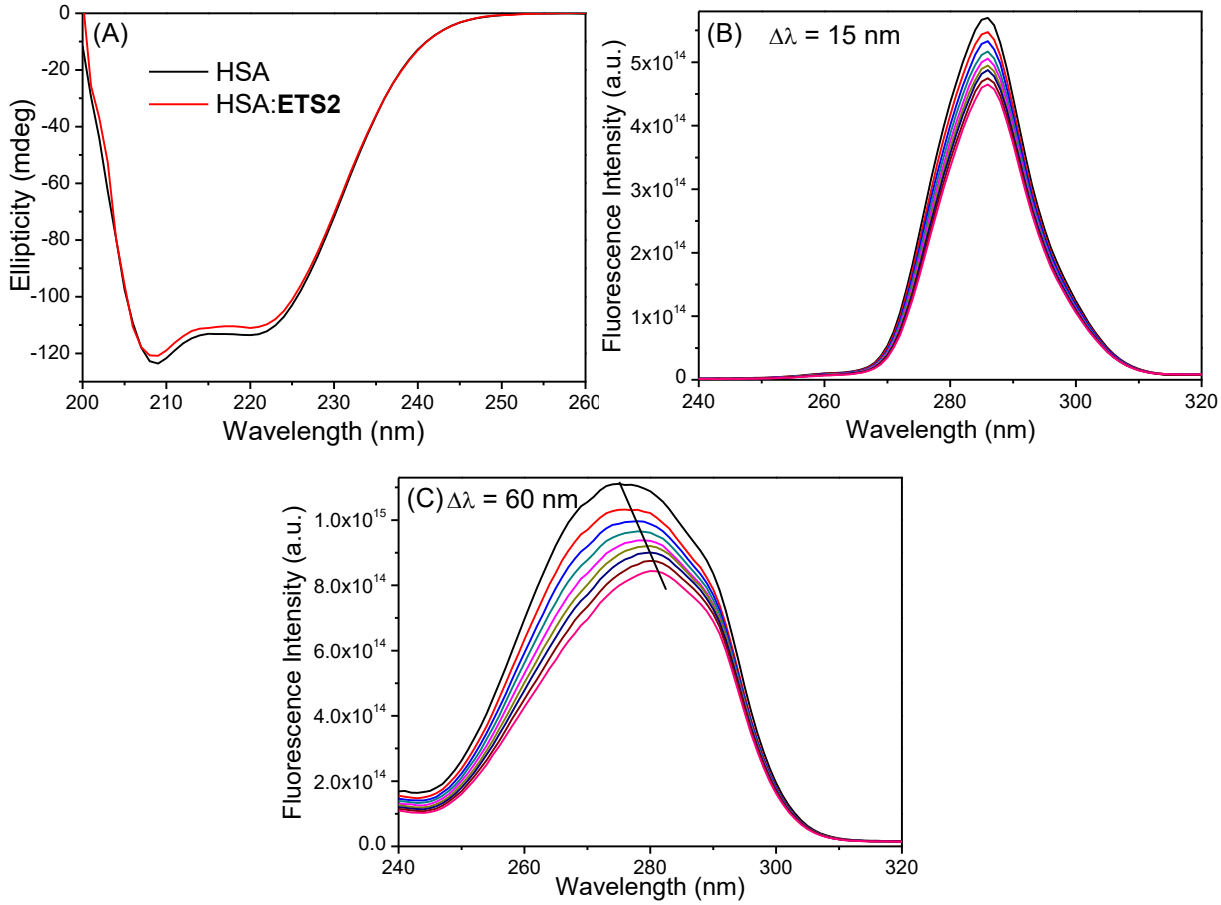

Figure 5. (A) CD spectra for the interaction HSA:**ETS2** at pH = 7.4 and 310 K. Synchronous fluorescence measurement for HSA without and with the presence of **ETS2** at Δλ = 15 nm (B) and Δλ = 60 nm (C). [HSA] = 1.00x10^{-5} M and [**ETS2**] = 0.17; 0.33; 0.50; 0.66; 0.83; 0.99; 1.15 and 1.32x10^{-5} M.

The quantitative α-helical content of free HSA, as well as bound to **ETS2** can be calculated from the molar residual ellipticity (MRE) values at 208 and 222 nm - equation 6 [16]:

(A)

$$\%\ \alpha\text{-}helix = \left[\frac{(-MRE_{208} - 4000)}{(33000 - 4000)}\right] x\ 100$$

(B) (6)

$$\%\ \alpha\text{-}helix = \left[\frac{(-MRE_{222} - 2340)}{30300}\right] x\ 100$$

where MRE_{208} and MRE_{222} are the observed MRE value at 208 and 222 nm, respectively; 4,000 and 2,340 are the MRE values of the β-form and random coil conformation cross at 208 and 222 nm respectively, and 33,000 and 30,300 are the MRE values of a pure α-helix at 208 and 222 nm, respectively [23,24]. Quantitatively, the α-helix percent decreases gradually, from 58.6% in free HSA to 57.4% upon **ETS2** binding, at 208 nm. Similarly, at 222 nm, the α-helix percent decreases gradually, from 55.6% in free HSA to 54.2%. The CD results indicate a very weak perturbation of the albumin structure upon binding with the **ETS2** ligand, indicating that binding does not affect significantly the α-helical content [25], a result similar to that found for **ETS1** [8].

Synchronous fluorescence (SF) spectroscopy is widely used to describe the interaction between a fluorescence quencher and proteins because it can provide information about the molecular environment in the vicinity of the functional fluorophore group. SF spectra are obtained by simultaneously scanning excitation and emission monochromators (Δλ). When Δλ = 15 and 60 nm characteristic information on the polarity in the microenvironment around tyrosine (Tyr) and tryptophan (Trp) residues, respectively, can be obtained [26]. SF spectra of HSA with different concentrations of **ETS2** at Δλ of 15 nm and 60 nm are shown in Fig 5.

The maximum fluorescence emission wavelength for the Tyr residue (Fig. 5B) shows no significant shift upon successive addition of **ETS2**, indicating that the microenvironment around this residue is not disturbed by the presence of the thiosemicarbazide under study [18].

On the other hand, there is a significant shift from 275 to 280 nm on the maximum emission wavelength for Δλ = 60 nm - Fig. 5C), which implies that interaction of **ETS2** with HSA affects the conformation of the region around the Trp residue [27]. This phenomenon was also observed for the thiosemicarbazide **ETS1** which does not contain the methyl group in its structure [8] and, therefore, both **ETS1** and **ETS2** affect weakly the secondary structure of the protein and the conformation in the region around the Trp residue.

Three-dimensional fluorescence spectroscopy (3D) can provide detailed information on the structural changes of the polypeptide backbone, as well as possible changes on the polarity of the microenvironment around the fluorophore residues through changes in the peak positions. 3D fluorescence spectra for HSA presents two peaks: peak I, which corresponds to π-π* transition of the C=O and peak II, which corresponds to π-π* transition of the fluorophores [28]. Peaks "a" ($\lambda_{ex} = \lambda_{em}$) and "b" ($2\lambda_{ex} = \lambda_{em}$) are referred as Rayleigh and second-order scattering peaks, respectively [29]. The corresponding 3D spectra and its contour map for HSA in the absence or in the presence of **ETS2** are shown in Fig. 6. As can be seen in the Table 2, the fluorescence intensity of peaks I and II decreases with the addition of **ETS2** - 5.59% and 4.45%, respectively. A weak change in the position of the emission wavelength (red Stokes' shift) may also be observed, suggesting possible perturbations in the polypeptide backbone as a result of the association between HSA and **ETS2** near the tryptophan residue [8]. These results are in full agreement with the SF and CD data already discussed above.

Table 2. 3D fluorescence spectral characteristics for HSA and HSA:**ETS2** at pH = 7.4 and room temperature.

System	Peak	Peak position ($\lambda_{exc}/\lambda_{em}$ nm/nm)	Intensity ($x10^3$) (a.u.)
HSA	a	225/225 → 350/350	27.4 → 15.2
	b	230/460	10.0
	I	280/330	17.9
	II	230/325	22.5
HSA: **ETS2**	a	225/225 → 350/350	21.5 → 15.0
	b	230/460	9.85
	I	280/335	16.7
	II	230/340	21.5

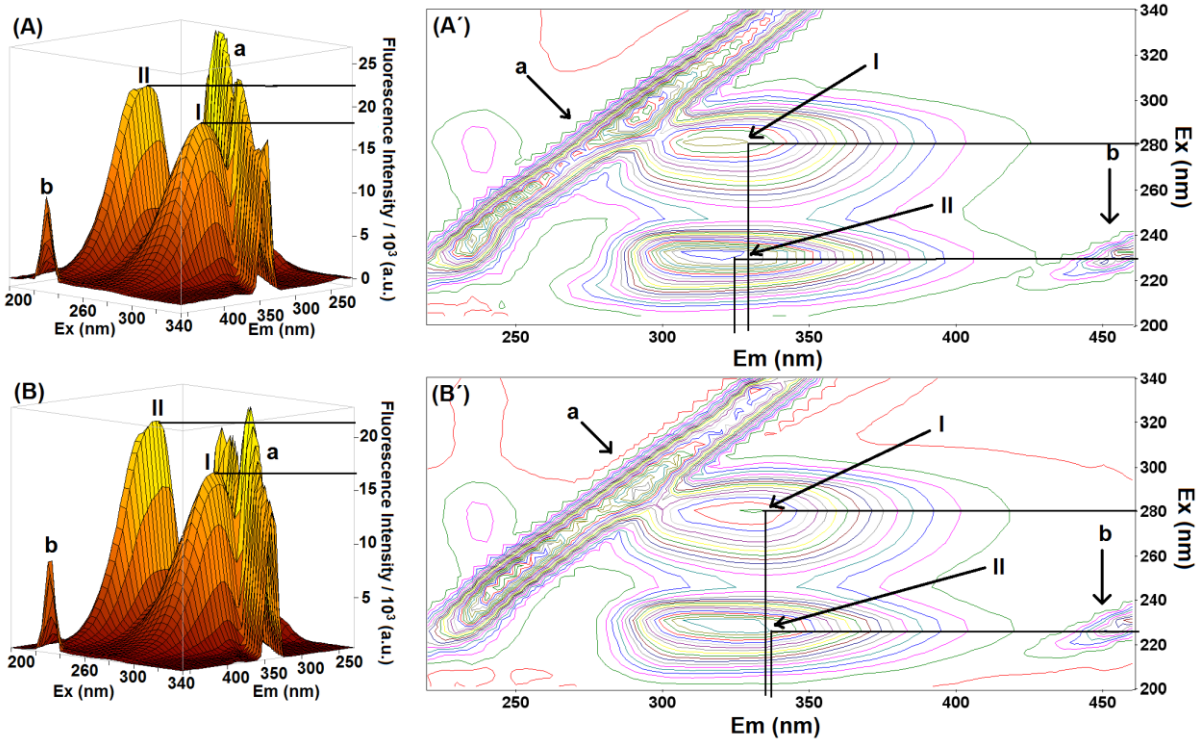

Figure 6. 3D fluorescence spectral projections and its and contour map for HSA (A and A´) and HSA:**ETS2** (B and B´) at pH = 7.4. [HSA] = 1.00x10^{-6} M and [**ETS2**] = 1.32x10^{-5} M.

Analysis of the main binding pocket of HSA to ETS2

There are three main binding sites located in HSA structure. Sudlow's site I is located in subdomain IIA (warfarin binding site), while Sudlow's site II is located in subdomain IIIA (ibuprofen binding site) and site III in subdomain IB (digitoxin binding site) [28,30]. Competitive binding studies were carried out in order to identify the main binding site in HSA structure to **ETS2**. The binding replacement was analyzed according to the modified Stern-Volmer plot (Fig. 7A). The calculated K_a values in the presence of warfarin, ibuprofen and digitoxin were (0.32±0.03)x10^4; (1.21±0.26)x10^4 and (1.26±0.26)x10^4 M^{-1}, respectively. Since the K_a value without and in the presence of warfarin changed significantly (77.1%), this is an indication of competition between warfarin and **ETS2** for the same binding site [31]. Thus, Sudlow's site I in subdomain IIA - where Trp-214 residue is located - is the main binding site for **ETS2**. The same binding site was also identified for **ETS1** [8].

The computational study by molecular docking is a common technique which is used efficiently to analyze the main intermolecular interactions between small molecules and macromolecules [28]. In order to offer more details about the interaction between **ETS2** and HSA inside Sudlow's site I, molecular docking exercise was carried out.

In agreement with the experimental results, molecular docking suggests that **ETS2** is able to be accommodated in the cavity next to the Trp-214 residue presenting a favorable interaction profile with the amino acid residues present in the cavity *via* hydrogen bonding and hydrophobic forces (Fig. 7B). One of the hydrogen atoms from the N-H group of the ligand structure is a potential donor for hydrogen bonding with the carboxyl group of Asp-450 residue, within a distance of 2.10 Å, while the hydroxyl group of Ser-453 residue is a donor for hydrogen bonding with the oxygen atom of the ligand structure within a distance of 2.10 Å. The fluorophore Trp-214 residue is hydrogen bonding with one of the nitrogen atoms from the **ETS2** structure within a distance of 3.60 Å, but not with the sulfur group as reported for **ETS1** [8]. Finally, molecular docking also suggests hydrophobic interactions between **ETS2** and the Ala-209, Val-342, Pro-446 and Leu-480 residues.

Overall, the molecular docking results suggest that the presence of the methyl group in the ligand structure changed the position of the thiosemicarbazide derivative inside albumin binding pocket, affecting mainly the interaction of Trp-214 and Asp-450 residues. The methyl group in the ligand structure interacts *via* hydrophobic forces with the Pro-446 residue.

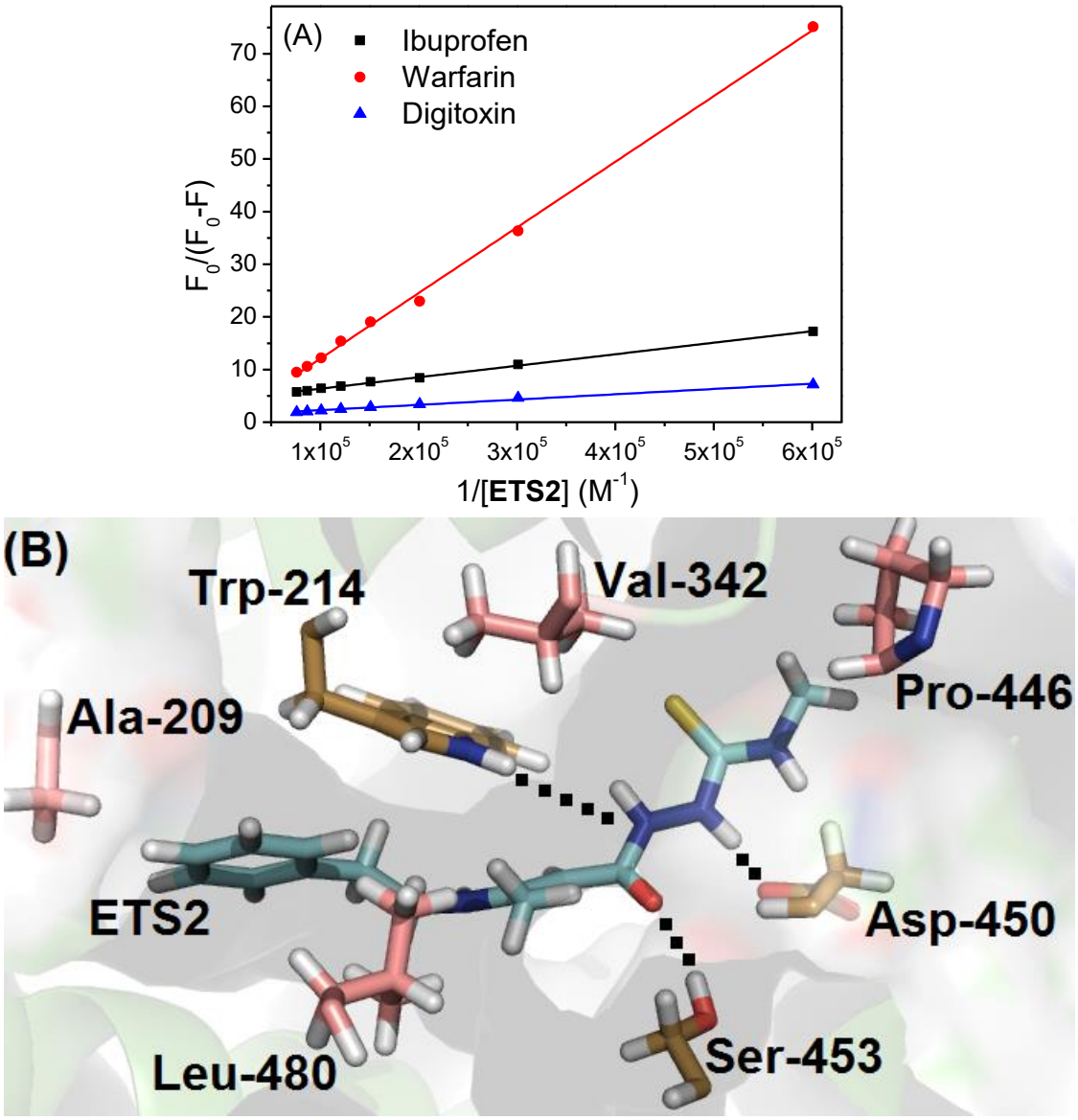

Figure 7. (A) Modified Stern-Volmer plots for the competitive binding studies in the presence of warfarin, ibuprofen and digitoxin at pH = 7.4 and 310 K. (B) Best molecular docking pose for the interaction between HSA and **ETS2** inside Sudlow's site I. Selected hydrophilic and hydrophobic amino acid residues and **ETS2** structure are represented in brown, beige and cyan, respectively. Hydrogen bonds are labeled as black dots. Hydrogen: white; oxygen: red; sulfur: yellow and nitrogen: dark blue.

Conclusions

The methyl thiosemicarbazide derivative **ETS2** binds moderately with HSA in Sudlow's site I (subdomain IIA) and causes a weak perturbation on the secondary structure of the albumin. The K_{SV}, k_q and fluorescence lifetime values suggested that the fluorescence quenching of the intrinsic fluorophore of the albumin (Trp-214) is *via* a static mechanism, indicating a ground state association HSA:**ETS2**. Thermodynamic parameters showed the spontaneity of the binding process ($\Delta G° < 0$), which is entropically driven ($\Delta S° > 0$). SF suggested that **ETS2** does not have any effect on the polarity around the Tyr residue; however, it can perturb the microenvironment around the Trp residue. Molecular docking results suggested hydrogen bonding and hydrophobic interactions as the main binding forces between **ETS2** and Ala-209, Trp-214, Val-342, Pro-446, Asp-450, Ser-453 and Leu-480 residues. Overall, **ETS2** can also be carried and biodistributed in the human bloodstream by the serum albumin. However, the experimental results showed that the presence of the methyl group in the ligand structure changed the thermodynamic profile, suggesting that this group decreases the binding ability towards serum albumin. Molecular docking suggested that the presence of the methyl group in **ETS2** changed the position of the thiosemicarbazide derivative inside the albumin binding pocket affecting mainly the interactions with the Trp-214 and Asp-450 residues, which were weakened.

Acknowledgments

The authors gratefully acknowledge the Brazilian agencies: Coordenação de Aperfeiçoamento de Pessoal de Nível Superior (CAPES), Conselho Nacional de Desenvolvimento Científico e Tecnológico (CNPq) and Fundação de Amparo à Pesquisa do Estado do Rio de Janeiro (FAPERJ) for financial support. The authors also acknowledge the collaboration of Prof. Nanci Câmara de Lucas Garden (UFRJ) for time-resolved, synchronous and 3D fluorescence facilities.

Conflict of Interest

The authors declare no conflict of interest.

References

1- S. Zhang, X. Chen, S. Ding, Q. Lei, W. Fang, Colloids Surf. A **2016**, 495, 30-38.
2- X. Li, S. Wang, New J. Chem., **2015**, 39, 386-395.
3- Reshma, S.K. Vaishnav, I. Karbhal, M.L. Satnami, K.K. Ghosh, J. Mol. Liq. **2018**, 255, 279-287.
4- O.A. Chaves, A.P.O. Amorim, L.H.E. Castro, C.M.R. Sant'Anna, M.C.C. de Oliveira, D. Cesarin-Sobrinho, J.C. Netto-Ferreira, A.B.B. Ferreira, Molecules **2015**, 20, 19526-19539.
5- E.J. Barreiro, C.A.M. Fraga, *Química Medicinal. As Bases Moleculares da Ação dos Fármacos*. 2nd Ed., Artmed, Porto Alegre, **2011**.
6- E.J. Barreiro, A.E. Kümmerle, C.A.M. Fraga, Chem. Rev. **2011**, 111, 5215-5246.
7- P. Bazzini, C.G. Wermuth, *The Practice of Medicinal Chemistry*. 4th Ed., Academic Press, San Diego, **2008**.
8- O.A. Chaves, M.R.L. Santos, M.C.C. de Oliveira, C.M.R. Sant'Anna, R.C. Ferreira, A. Echevarria, J.C. Netto-Ferreira, J. Mol. Liq. **2018**, 254, 280-290.
9- O.A. Chaves, C.S.H. Jesus, P.F. Cruz, C.M.R. Sant'Anna, R.M.M. Brito, C. Serpa, Spectrochim. Acta Mol. Biomol. Spectrosc. **2016**, 169, 175-181.
10- I. Matei, S. Ionescu, M. Hillebrand, J. Lumin. **2011**, 131, 1629-1635.
11- M. Wardell, Z. Wang, J.X. Ho, J. Robert, F. Ruker, J. Ruble, D.C. Carter, Biochem. Biophys. Res. Commun. **2002**, 291, 813-819.
12- http://www.ccdc.cam.ac.uk/solutions/csd-discovery/components/gold/, accessed February 2018.
13- S. Yasmeen, Riyazuddeen, J. Mol. Liq. **2017**, 233, 55-63.
14- S. Karthikeyan, G. Bharanidharan, M. Kesherwani, K.A. Mani, N. Srinivasan, D. Velmurugan, P. Aruna, S. Ganesan, J. Biomol. Struct. Dyn. **2016**, 34, 1264–1281.
15- Z. Tian, F. Zang, W. Luo, Z. Zhao, Y. Wang, X. Xu, C. Wang, J. Photochem. Photobiol. B Biol. **2015**, 142, 103–109.
16- O.A. Chaves, E. Schaeffer, C.M.R. Sant'Anna, J.C. Netto-Ferreira, D. Cesarin-Sobrinho, A.B.B. Ferreira, Mediterr. J. Chem. **2016**, 5, 331-339.
17- H. Sun, Y. Liu, M. Li, S. Han, X. Yang, R. Liu, Luminescence **2016**, 31, 335-340.
18- S. Bi, T. Zhao, H. Zhou, Y. Wang, Z. Li, J. Chem. Thermodynamics **2016**, 97, 113-121.
19- O.A. Chaves, D. Cesarin-Sobrinho, C.M.R. Sant'Anna, M.G. Carvalho, L.R. Suzart, F.E.A. Catunda-Junior, J.C. Netto-Ferreira, A.B.B. Ferreira, J. Photochem. Photobiol. A: Chem. **2017**, 336, 32-41.
20- F. Shiri, S. Shahraki, A. Shahriyar, M.H. Majd, J. Photochem. Photobiol. B **2017**, 170, 152–163.
21- X. Zhang, R. Gao, D. Li, H. Yin, J. Zhang, H. Cao, X. Zheng, Spectrochim. Acta Mol. Biomol. Spectrosc. **2015**, 136, 1775-1781.
22- P.D. Ross, S. Subramanian, Biochemistry **1981**, 20, 3096-3102.
23- W. Zhang, F. Wang, X. Xiong, Y. Ge, Y. Liu, J. Chil. Chem. Soc. **2013**, 58, 1717-1721.
24- A. Varlan, M. Hillebrand, Molecules **2010**, 15, 3905-3919.
25- O.A. Chaves, L.S. Barros, M.C.C. de Oliveira, C.M.R. Sant'Anna, A.B.B. Ferreira, F.A. Silva, D. Cesarin-Sobrinho, J.C. Netto-Ferreira, J. Fluor. Chem. **2017**, 199, 30–38.
26- X. Ma, J. Yan, K. Xu, L. Guo, H. Li, Bioorg. Chem. **2016**, 66, 102-110.
27- Z. Sun, H. Xu, Y. Cao, F. Wang, W. Mi, J. Mol. Liq. **2016**, 219, 405-410.
28- B. Tang, Y. Huang, X. Ma, X. Liao, Q. Wang, X. Xiong, H. Li, Food Chem. **2016**, 212, 434-442.
29- A.N. Nasruddin, S.R. Feroz, A.K. Mukarram, S.B. Mohamad, S. Tayyab, J. Lumin. **2016**, 174, 77-84.
30- G. Sudlow, D. J. Birkett, D. N. Wade, Mol. Pharmacol. **1976**, 12, 1052-1061.
31- K. Paal, A. Shkarupin, L. Beckford, Bioorg. Med. Chem. **2007**, 15, 1323-1329.